Plate Modal and Lateral Vibration Displacement Sensors

Aniket Pinjan and Marcellin Zahui

Abstract— Plate vibration characteristics such as mode shapes and deflections or natural frequencies and damping factors can be measured with accelerometers, laser based systems, and other sensing technologies. The work presented in this paper is about the direct measurement of the deflection curve of a vibrating plate using piezoelectric films. The sensor consists of an array of PolyVinyliDene Fluoride (PVDF) film patches bonded to the surface of the plate. The patches are oriented such that the piezoelectric axis 1 is along the plate axis of interest to minimize the effect of the strains from the piezoelectric axis 2. These right angle quadrilaterals patches are etched on the film electrode to create multiple separate sections of the sensor. The output charge of each patch is proportional to the plate deflection slope at the center of the patch in the direction of the axis coinciding with the piezoelectric axis 1. The plate lateral displacement elevations are calculated from these slopes using central difference formulas. In this paper, the equations of the sensor are derived for the general vibration case and for the particular case of resonance vibration of the plate. The work is validated with numerical simulation and limited experimental results. The numerical simulation is performed using modes superposition techniques applied to a simply supported and a clamped plate while only a clamped plate is used in the experimental verification. The results indicate that the proposed sensor can be used to effectively measure the lateral vibration displacement curves of plates with various boundary conditions.

Index Terms— Displacement sensors, Control systems, Modal analysis, Plate vibration, PVDF, Sensor, Vibration.

1 Introduction

SENSORS Sensors and actuators are critical components of many Industrial applications including vibration and noise control, structure health monitoring, and many others. For example, in some active noise control applications, microphones are used to provide error signal necessary for the loudspeaker actuators to perform the noise cancelation [1]. Piezoelectric films [2], especially PolyVinyliDene Fluoride (PVDF) films have been at the forefront of actuators and sensors development. PVDF is a piezoelectric polymer that can be manufactured in micrometer [3] size flexible and resilient films. The PVDF films can also be easily cut into or etched in desired patterns [4]. These properties make them suitable for sensor development because they add little loading to the receiving structure. For actuator application, the films are often bonded in multiple layers in order to increase the total actuation force.

The use of PVDF films as sensors or actuators can be found in literature across a wide range of applications such as active noise and vibration control [5], Material characterization6, Medical field [7] etc. The PVDF is usually in the form of film bonded to the structure [8] or embedded in a standalone sensor. PVDF film configured as vibrating membrane was recently used for actuation in fatigue testing of thin films [9]. Laminates of PVDF film were also used as actuators to control the vibration of a cylindrical shell [10]. As previously stated, multiple layers of film are often used to increase the available actuating force. However, for sensing, the ideal situation is to use as minimum number of layers as possible so that the sensor does not interfere with the structure's dynamic properties. In general the film is very flexible compared to the structure to which it is bonded therefore the effect of the film on the structure is expected to be very small. Shaped films [11] have been extensively used to measure the dynamic properties of flexible structures. For instance, beams and plates volume velocity were previously measured for active noise and vibration cancellation [12] using quadratic functions to shape the piezoelectric film sensors. Other researchers have used a mixture of quadratic and linear functions to shape sensors for local volume velocity [13] cancelation applications.

In this paper, we propose to measure the lateral displacements of a vibrating plates of various boundary conditions using distributed sensors. Generally, point sensors such as accelerometers or laser vibrometers are used to measure the dynamic properties of vibrating structures. However, for many industrial applications that require full continuum data and minimum delay in the measurement, point sensors are often cumbersome and computation intensive. For example the measurement of the vibration curve of a beam will require multiple accelerometers with individual signal conditioners and a software to process the data from all the accelerometers. Thus, researchers have been looking for more non-conventional sensors, mainly distributed sensors to reduce delay in the control loops or capture full structure continuum dynamic properties. In the case of active noise or vibration control, distributed sensors will usually provide better measurement of the vibration properties of the controlled structure. Furthermore, distributed sensors can give simultaneous measurement data at multiple locations on the structure therefore elimi-nate the need for extrapolation. Another downside of point sensors is for example, a point sensor on a relatively long vibrating beam could provide a false reading if the sensor is located at a node [14].

The proposed sensor could be used at low cost to monitor the structural supports of signs, luminaires, and traffic signals [15] for streets or highways. Various vibration mitigation devices have been proposed and implemented on these support struc-tures. However, their effectiveness has not been assessed on a continuous basis. The proposed sensor could be an affordable solution for evaluating and monitoring the effectiveness of

the vibration-mitigation [16] devices of these support structures. Another motivation for the current work is the measurement of impact loadings on snowmobile ruining boards and handle bars. In the case of the running board application, the proposed sensor can be used in a force plate to measure the amplitude and location of the impact force from the riders' feet.

The sensor discussed herein can also be used in active vibration and noise control or structural members health monitoring. The film can be bonded on the surface of a plate or embed-ded within the layers of a composite plate to measure the real time instantaneous vibration shapes of the plate. Other plate mechanical properties such as strains and stresses can be deter-mined from the measured deflections. Thus, making the pro-posed sensor an invaluable asset in active structural control or structural health monitoring. Furthermore, dynamic properties such as natural frequencies and mode shapes can also be calculated from the measured deflection curves.

PVDF films are piezoelectric strain sensors that do not require any external power supply unlike strain gauges. Dynamic sensors using strain measurement techniques have been around for decades. They use internal beams [17] to measure the dynamic properties of the structure under test from the strain on the surface of the beam. A cantilever beam with a mass at the free end is often used taking advantage of the fact that the strain at any point along the beam is proportional to the motion of the mass. The motion of the mass is then related to the dis-placement of the base and the motion of the corresponding point on the structure under test. The proposed sensor extends the concept described above but, the PVDF strain sensor is directly attached to the structure under test. Therefore, using mul-tiple patches of the film, the strains at multiple locations on the plate can be measured. These strains are converted by the film into electrical charges that are proportional to the slopes at the patch locations, and thus, the strains are translated into displacements of the surface of the vibrating plate. Consequently, the accuracy of the measurement will depends on the number of sensor patches relative to the highest frequency [18] of interest in the measurement. In practice, useful structures have relatively long vibration flexural wavelengths, hence, a large number of sensor patches is not usually needed.

The displacement sensor approach presented here is made possible by the availability and cost of PVDF films, etching processes, and single chip computers. These sensors breaks with the traditional sensor design concept whereby the sensing and the processing units are separate. In the proposed sensor technology, a working sensor will also include the data processing capability. An example of that would be an accelerometer with embedded chip for signal processing.

The paper is structured as follows. The sensor design section presents the general equation of PVDF film bonded to arbitrary structures followed by beams and plates vibration displacement sensor equations. The numerical simulation section is used to describe the equations and the process used to compare dis-placements calculated using mode superstition on one hand and displacements calculated using sensor equations on the other hand. The final section is devoted to the experimental procedures and results. Summary remarks and applications notes are presented in the conclusion.

2 Sensor Development

2.1 Derivation of Piezoelectric Film Output Charge Equations

In this section, we consider a piezoelectric film bonded to a generic flexible structure. The flexible structure continuum surface is totally covered by the film. Thus, to derive the piezoelectric equations, we will make the following assumptions. (1) The film is much thinner than the flexible structure therefore the strains in the film are assumed to be the same as in the substrate outer surface. (2) The piezoelectric film is perfectly coupled with the flexible structure without changing the dynamic characteristics such as natural frequencies and mode shapes of the structure. Under these assumptions, we should only consider the transverse electric field of the film. Using direct piezoelectric equations for linear piezoelectricity [19] and Figure 1 the voltage across the electrodes can be written as shown in Equation (1)

$$\phi_3 = -\int^{h_f} E_3 d\alpha_3 \tag{1}$$

where h_f is the piezoelectric film layer thickness. From Figure 1, the above equation can be expressed in term of normal strains in the film S_{11}^f and S_{22}^f in the direction of α_1 and α_2 respectively, and the electric displacement vector D_3.

$$\phi_3 = h^f \left(h_{31} S_{11}^f + h_{32} S_{22}^f - \beta_{33} D_3 \right) \tag{2}$$

where β_{33} and h_{ij} represent respectively the impermeability and the strain charge coefficients of the piezoelectric film. Equation (1) is the output voltage of the film so it can be integrated over the entire film surface. This yields the following equation:

$$\begin{aligned}\phi(\alpha_1,\alpha_2) = \frac{h^f}{S^f}\int_{S^f} & h_{31}\left\{\left[\frac{1}{A_1}\frac{\partial u_1}{\partial \alpha_1}+\frac{u_2}{A_1A_2}\frac{\partial A_1}{\partial \alpha_2}+\frac{u_3}{R_1}\right]\right. \\ & + r_1^f\left[\frac{1}{A_1}\frac{\partial}{\partial \alpha_1}\left(\frac{u_1}{R_1}-\frac{1}{A_1}\frac{\partial u_3}{\partial \alpha_1}\right)\right. \\ & \left.\left.+\frac{1}{A_1A_2}\frac{\partial A_1}{\partial \alpha_2}\left(\frac{u_2}{R_2}-\frac{1}{A_2}\frac{\partial u_3}{\partial \alpha_2}\right)\right]\right\} \\ & + h_{32}\left\{\left[\frac{1}{A_2}\frac{\partial u_2}{\partial \alpha_2}+\frac{u_1}{A_1A_2}\frac{\partial A_2}{\partial \alpha_1}+\frac{u_3}{R_2}\right]\right. \\ & + r_2^f\left[\frac{1}{A_2}\frac{\partial}{\partial \alpha_2}\left(\frac{u_2}{R_2}-\frac{1}{A_2}\frac{\partial u_3}{\partial \alpha_2}\right)\right. \\ & \left.\left.\left.+\frac{1}{A_1A_2}\frac{\partial A_2}{\partial \alpha_1}\left(\frac{u_1}{R_1}-\frac{1}{A_1}\frac{\partial u_3}{\partial \alpha_1}\right)\right]\right\}\right] dS^f\end{aligned} \tag{3}$$

where u_1, u_2, and u_3 are the flexible structure displacements in the three principal direction of α_1, α_2, and α_3 respectively. r_1^f and r_2^f represent respectively the distances from the neutral

surface to the bottom and top plane of the piezoelectric film layer. S is the structure or film area. Finally A_1 and A_2 are the Lamé parameters [20] from the fundamental equation

$$(ds)^2 = A_1^2 (d\alpha_1)^2 + A_2^2 (d\alpha_2)^2 \quad (4)$$

Considering Equation (3), Zou showed that the output of the piezoelectric film can be calculated analytically for simple structures such as beam and plates if u_1, u_2, and u_3 are known. However, for complex structures and boundary conditions, analytical solution is impossible and one must resort to numerical simulations.

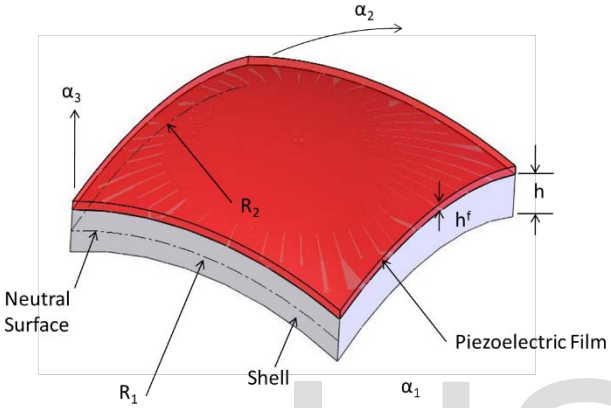

Fig. 1. Shell covered with PVDF film.

2.2 Plate Flexible Structure

For In this case, the film is bonded to a plate undergoing transverse motion such that $R_1 = R_2 = \infty$. The Lamé parameters are derived from the fundamental equation $(ds)^2 = (1)^2 (dx)^2 + (1)^2 (dy)^2$ and therefore $A_1 = A_2 = 1$. Substituting these values into Equation (3) and setting $z = u_3$ gives the piezoelectric film output voltage as:

$$\phi = -\frac{h^f}{S^f} \int_{S^f} \left[h_{31} r_x^f \frac{\partial^2 z}{\partial x^2} + h_{32} r_y^f \frac{\partial^2 z}{\partial y^2} \right] dS^f \quad (5)$$

2.3 Plate Flexible Structure

Equation (5) can be further simplified if only one axis is considered. This leads to the charge equation of the film bonded to a beam when the term h_{32} is removed and $dS^f = bdx$ where b is the width of the beam.

$$\phi = -\frac{bh^f}{S^f} \int_x \left(h_{31} r_x^f \frac{\partial^2 z}{\partial x^2} \right) dx \quad (6)$$

2.4 Sensor Equation

2.4.1 Beam Displacement Sensor Equation

The design and implementation of the beam lateral vibration displacement sensor can be found in [21] and [22]. The theory of the bean sensor is briefly reported here to provide insight in the design and development of the plate lateral vibration displacement sensor. If we consider a beam substrate and use multiple patches of film as shown in Figure 2 with n segments of films, the i^{th} patch output charge can be written from Equation (6) in the form of:

$$\phi_i = -\frac{bh^f_i}{S_i^f} \int_{x_{i-1}}^{x_i} \left(h_{31_i} r_{x_i}^f \frac{\partial^2 z_i}{\partial x^2} \right) dx, \quad (7)$$

after integration, Equation (7) yields:

$$\phi_i = -\frac{bh^f_i}{S_i^f} h_{31_i} r_{x_i}^f \left[\frac{\partial z_i}{\partial x} \right]_{x_{i-1}}^{x_i}. \quad (8)$$

If we assume that the slope of the beam deflection is constant at the location of the i^{th} patch and set equal to z_x^i, then Equation (8) can be written as:

$$\phi_i = -\frac{bh^f_i}{S_i^f} h_{31_i} r_{x_i}^f z_x^i. \quad (9)$$

The above equation shows that the i^{th} film patch output signal is proportional to the slope of the displaced patch. Then the slope z_x^i can be written in term of the i^{th} patch output charge ϕ_i.

$$z_x^i = -\frac{\phi_i S^f_i}{bh_i^f h_{31_i} r_{x_i}^f}. \quad (10)$$

Equation (9) represents the sensor general equation from which the slope of the beam section at the location of the sensor patch can be calculated using Equation (10).

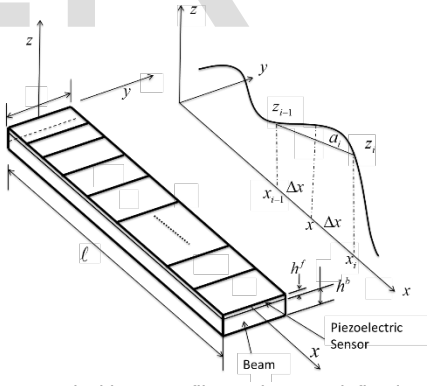

Fig. 2. Beam covered with PVDF film and Beam deflection curve.

2.4.2 Beam Lateral Displacement Equation

The function z shown in Figure 2 represents the deflection of the beam. It can be evaluated at points that lie to the left and right of the center point x of the i^{th} patch. Thus, the central-difference formula for the slop z_x at the center of the patch is found through the following equation

$$z_x^i \cong \frac{z(x+\Delta x) - z(x-\Delta x)}{2\Delta x} \quad (11)$$

Setting $z_{i-1} = z(x-\Delta x) = z(x_{i-1})$, $z_i = z(x+\Delta x) = z(x_i)$, and $2\Delta x = x_i - x_{i-1}$ the above equation becomes

$$z_i \cong z_x^i (x_i - x_{i-1}) + z_{i-1} \tag{12}$$

The combination of Equation (10) and Equation (12) can be further simplified. If, for practical purposes, we assume that the piezoelectric patches are of equal sizes and fabricated from the same uniform thickness film such that:

$$x_i - x_{i-1} = \frac{\ell}{n},\ r_{x_i}^f = \frac{h^f + h^b}{2} \cong \frac{h_b}{2},\ h_{31_i} = h_{31}\ , \tag{13}$$

Then Equation (12) can be written as

$$z_i = -2\frac{\phi_i \ell^2}{h^f h_s h_{s_i} n^2} + z_{i-1} \tag{14}$$

The above Equation (14) represents the general form of the beam lateral displacement equation and is independent of the beam boundary conditions. However z_0 must be known to calculate the rest of the values in the series. Therefore the requirement on this method is that the displacement of at least one end of the beam must be known. For clamped and simply supported boundary conditions, the vector $\{z\}$ of z_i represents an approximation of the curve shown in Figure 2. For any other boundary conditions, a point sensor near the boundary can be used to find z_0 and the rest of the elements of the series.

2.4.3 Plate Displacement Sensor Equation

For the plate vibration displacement sensor, plate substrate and Equation (5) is considered. Figure 3 shows a plate with multiple patches of film where the red grid represents the patches while the dotted grid is used to locate the center of the patches and provide two indexes ij to reference the patch. Thus the plate is covered with $p \times q$ patches of films. The ij patch output charge can be written as:

$$\phi_{ij} = -\frac{h_{ij}^f}{S_{ij}^f} \int_{x_{j-1}}^{x_j} \int_{y_{i-1}}^{y_i} \left[h_{31} r_x^f \frac{\partial^2 z}{\partial x^2} + h_{32} r_y^f \frac{\partial^2 z}{\partial y^2} \right] dxdy \tag{15}$$

The charge ϕ_{ij} can be calculate by separating the equation into two:

$$\phi_{ij}^x = -\frac{h_{ij}^f}{S_{ij}^f} \int_{x_{j-1}}^{x_j} \int_{y_{i-1}}^{y_i} h_{31} r_x^f \frac{\partial^2 z}{\partial x^2} dxdy \tag{16}$$

$$\phi_{ij}^y = -\frac{h_{ij}^f}{S_{ij}^f} \int_{x_{j-1}}^{x_j} \int_{y_{i-1}}^{y_i} h_{32} r_y^f \frac{\partial^2 z}{\partial y^2} dxdy \tag{17}$$

The integration of Equation (16) along $x-$direction and Equation (17) along the $y-$direction yields the following equations:

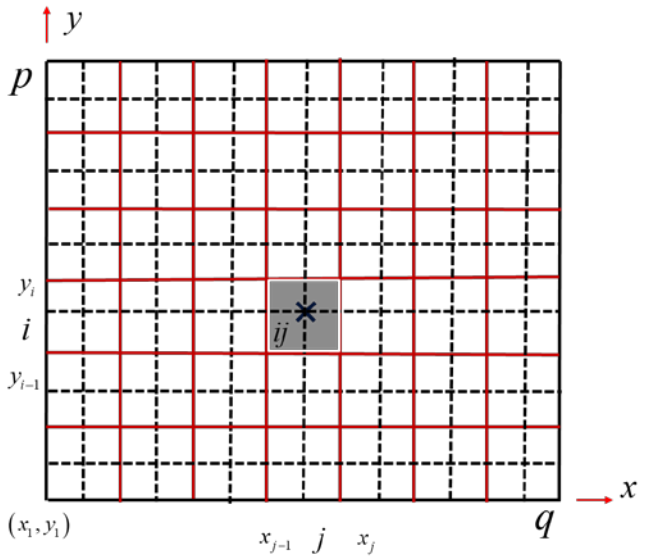

Fig. 1. Plate covered with PVDF film for general vibration case.

$$\phi_{ij}^x = -\frac{h_{ij}^f}{S_{ij}^f} \int_{y_{i-1}}^{y_i} h_{31} r_x^f \left[\frac{\partial z}{\partial x} \right]_{x_{j-1}}^{x_j} dy \tag{18}$$

$$\phi_{ij}^y = -\frac{h_{ij}^f}{S_{ij}^f} \int_{x_{j-1}}^{x_j} h_{32} r_y^f \left[\frac{\partial z}{\partial y} \right]_{y_{i-1}}^{y_i} dx \tag{19}$$

The slopes $z_x^{ij} = \partial z/\partial x$ in the $x-$direction and $z_y^{ij} = \partial z/\partial y$ in the $y-$direction are respectively assumed constant at the location of the ij^{th} patch. These equation are similar in form to Equation (8) but their dependency on the gradient in the $y-$direction for Equation (18) and $x-$direction for Equation (19) complicates the integration. In practice, sensor strip laid as the blue area shown in Figure 4 where the sensor patch piezoelectric $1-$ axis is lined up with the $x-$ axis and the $y-$dimension is much smaller than the $x-$ dimension, the output charges will account more for strains in the $x-$ direction than in the $y-$direction. Similar observation can be made for the green film strip by reversing the x & y axis.

Now using Raleigh formulation, the mode shapes of a plate can be written as the product of beam functions:

$$W(x,y) = X(x)Y(y) \tag{20}$$

where $X(x)$ and $Y(y)$ are chosen as the fundamental mode shapes of beams having the boundary conditions of the plate [23] This formulation works well for all plates boundary condition except for free edges where approximate solution is required. Therefore the following discussion will focus on plates with clamped or simply supported edges. First we will consider a case where the plate is vibrating at one of its fundamental frequencies and second we will derive equations for the general case of plate vibration.

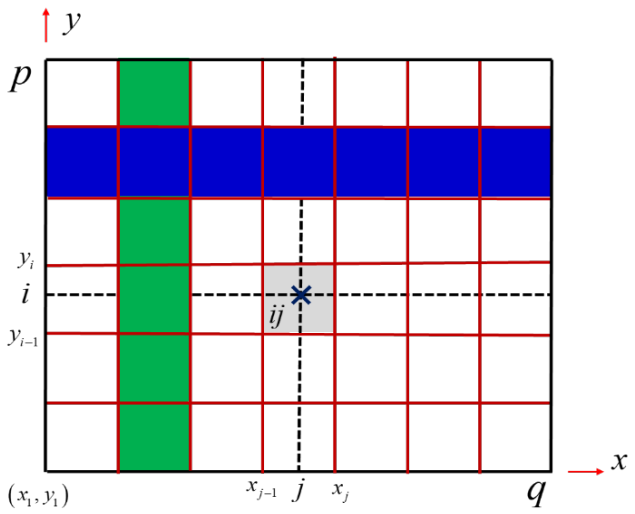

Fig. 2. Plate with two PVDF film strips for vibration at resonance.

Using Raleigh formation and Figure 4 the sensor strips respectively along the $x-$ and $y-$ directions, the output charges can be written as in Equation (9):

$$\phi_j^x = -\frac{h_j^f \Delta y}{S_j^f} h_{31_j} r_{x_j}^f z_x^j \tag{21}$$

$$\phi_i^y = -\frac{h_i^f \Delta x}{S_i^f} h_{31_i} r_{x_i}^f z_y^i \tag{22}$$

Where Δy and Δx are respectively sensor width for the sensor along the $x-$direction and $y-$ direction. Based on the beam sensor theory, the plate deflection z_j^x and z_i^y along the PVDF strips can be written as

$$z_j^x \cong z_x^j (x_j - x_{j-1}) + z_{j-1}^x \tag{23}$$

$$z_i^y \cong z_y^i (y_i - y_{i-1}) + z_{i-1}^y \tag{24}$$

where z_x^j and z_y^i are respectively calculated from ϕ_j^x and ϕ_i^y. From Raleigh formulation, the deflection of the plate is given by the following equation.

$$z(x,y) \cong z^x z^y \tag{25}$$

Equation (25) is only valid when the plate is vibrating at one of its fundamental frequencies because at resonance, the shape of the plate along the $x-$ direction remains constant across the $y-$direction while the shape of the plate along the $y-$direction remains constant across the $x-$ direction. For an off resonance vibration of the plate however, these two sensor strips will only capture the deflections at their locations and Equation (25) cannot be used.

For plate vibrating off resonance, multiple blue and green film strips can be used such that there will be at each ij location two superposed top and bottom patches. Therefore at a given ij location we can measure the slope in the $x-$ direction as z_x^{ij} and the slope z_y^{ij} in the $y-$ direction. From these two measured slopes at ij we can calculate the mixed partial derivative z_{xy}^{ij} as $z_x^{ij} z_y^{ij}$. The deflection z^{ij} at the location ij can then be calculated using the central difference equation for mixed partial derivative as follows:

$$z_{xy}^{ij}(x_j, y_i) \approx \frac{1}{2\Delta x \Delta y}\left(z_{i,j} - z_{i-1,j} + z_{i,j-1} - z_{i-1,j-1}\right) \tag{26}$$

The indices begin at 1 and the equation is written such that row $i=1$ corresponds to $y=0$ and column $j=1$ correspond to $x=0$ in the (x,y) coordinates system. Therefore, from Equation (26), it is clear that if the boundary conditions $z_{1,?}$ and $z_{?,1}$ respectively along the $x-axis$ and $y-axis$ are known, the deflection z_{ij} at ij can be calculated. The PVDF film arrangement described here can be used to effectively measure the lateral vibration displacement curve of a plate. This arrangement calls for fully covering the plate with bands of film in the $x-$ and $y-$ direction and thus two layers of film are required [24].

Another approach is to use a set of films either is the $x-$ direction or $y-$ direction eliminating the need to use two layers. In this case Equation (21) or Equation (22) is used respectively in $x-$ or $y-$ direction by properly orienting film piezoelectric direction 1. The displacement of the plate can then be calculated by applying Equation (23) or (24) along each sensor strip.

3 Numerical Simulation

The plate displacement sensor presented above is validated in this section with MATLAB numerical simulation. The data of Table 1 and Table 2 is used in the simulation to verify Eqs. (23) and (25). First the sensor for the vibration of the plate at resonance is implemented for a selected set of fundamental frequencies. Then, an arbitrary off resonance frequency is used with off-resonance sensor configuration to show that the sensor can measure the plate lateral displacement at any frequency or in a general vibration case.

Arbitrary selected modes $(1,1),(1,2),(2,1),\&(2,2)$ for the mode shape couple (n,m) are used to calculate the "actual" or theoretical deflections of the plate using Equation (27) for the simply supported plate and Equation (28) for the clamped plate.

TABLE 1
GEOMETRY AND PHYSICAL CONSTANTS FOR THE PLATE.

Plate		
Parameter	**Value**	**Units**
Length	610	*mm*
Width	381	*mm*
Thickness	4.76	*mm*
Mass density	2700	Kg/m^3
Young's modulus	70E9	N/m^2
Poisson ratio	0.33	...

Table 2
GEOMETRY AND PHYSICAL CONSTANTS THE PVDF FILM.

PVDF		
Parameter	**Value**	**Units**
Thickness	28	μm
Mass density	1780	Kg/m^3
Young's modulus	2.3E9	N/m^2
Stress/charge constant h_{31}	0.310	$V/m/N/m^2$
Stress/charge constant h_{32}	0.025	$V/m/N/m^2$
Stress/charge constant h_{33}	…	...

$$z(x,y) = C_{nm}\left[\sin(\beta_n x)\right]\left[\sin(\beta_m y)\right] \quad \text{with } \sin\beta_n L_x = 0 \text{ and } \sin\beta_n L_y = 0 \tag{27}$$

$$z(x,y) = C_{nm}\left[\sinh\beta_n x - \sin\beta_n x + \alpha_n(\cosh\beta_n x - \cos\beta_n x)\right]\times \left[\sinh\beta_m y - \sin\beta_m y + \alpha_m(\cosh\beta_m y - \cos\beta_m y)\right]$$

with

$$\cos\beta_n L_x \cos\beta_n L_x = 1 \text{ and } \alpha_n = \left(\frac{\sinh\beta_n L_x - \sin\beta_n L_x}{\cos\beta_n L_x - \cosh\beta_n L_x}\right) \tag{28}$$

$$\cos\beta_m L_y \cos\beta_m L_y = 1 \text{ and } \alpha_m = \left(\frac{\sinh\beta_m L_y - \sin\beta_m L_y}{\cos\beta_m L_x - \cosh\beta_m L_y}\right)$$

where C_{nm} is an amplitude factor. Then using the blue and green strips shown on Figure 4, the output charges ϕ_j^x and ϕ_i^y are calculated from Equation (7) respectively along the $x-$ and $y-$ axis. These charges are related to the deflection slopes z_x^j and z_y^i which are calculated before the deflections z_j^x and z_i^y are calculated using Eqs. (23) and (24). Finally the plate "measured" lateral displacement curve is calculated using Equation (25). Figures 5 for simply supported and 6 for clamped plates show the plate lateral deflection plots of the "Actual" or theoretical and "Measured" or calculated from PVDF charges. The results, shown in Figure 5 for the simply supported plate and Figure 6 for the camped plate, indicate that the PVDF sensor strips arrangement proposed here can be used to not only validate the Raleigh formulation of the mode shapes of vibrating plates but also the measurement of the lateral plate deflection theory presented for plate vibrating at resonance.

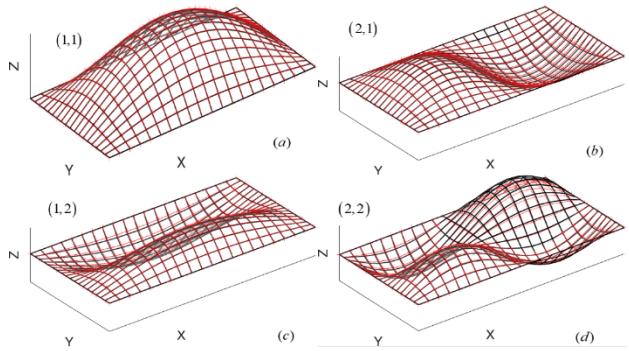

Fig. 3. Simply supported plate displacement at resonance (Black="Actual", Red="Measured").

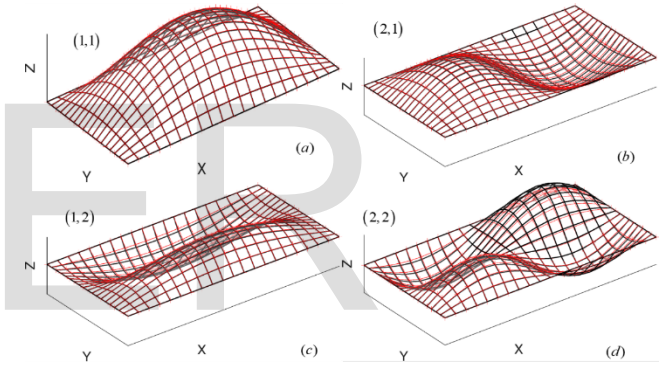

Fig. 4. Clamped plate displacement at resonance (Black="Actual", Red="Measured").

For off resonance simulation of the vibrations of the plate, mode superposition is used with the shape functions of Equation (27) for simply supported plate and Equation (28) for clamped plate. The four arbitrary shape functions $(1,1),(1,2),(2,1),\&(2,2)$ are used with random mode participation factors. The resulting equation is used to calculate the theoretical or "Actual" plate deflections. Then assuming that multiple blue filmstrips shown in Figure4 are used, the slopes z_x^{ij} are calculated with Equation (21) from the patches output charges after the charges have been calculated from Equation (7). The "measured" lateral displacements of the plate are finally calculated using Equation (23). Ones again the results shown in Figure 7 indicate that the proposed sensor can be utilized to effectively measure the displacement curve for general vibration case of plates.

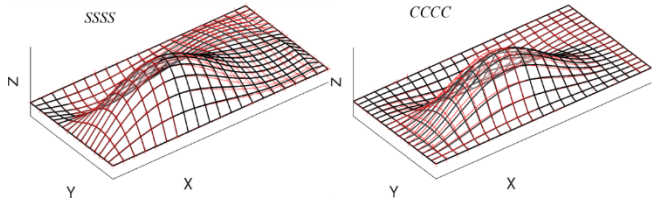

Fig. 5. Plate displacement off resonance (Black="Actual", Red="Measured").

4 Experimental Verification

To verify the proposed sensor theory ~~presented~~ and numerically simulated above, the experimental setup of Figure (8) is constructed. The plate is made of 4.76 mm-thick, 609.6 mm-long, and 381 mm-wide aluminum and clamped on each edge over 15 mm making the surface of the plate free to vibrate 594.6 mm by 366 mm. The sensor is fabricated out of $28\mu m$ thick copper-nickel metallized PVDF film. The fabrication process can be found in reference [22]. The sensor strips are bonded to the plate with a double sided high strength adhesive tape after the discontinuity between the patches is checked to ensure that they are electrically isolated from each other. An important step of this process is the surface preparation. The surface preparation involves degreasing of the plate surface followed by wet abrading using a medium grit sandpaper and then a fine grit sandpaper. Next, a conditioning solution is used to thoroughly clean the surface. Once the surface is cleaned, a neutralizing solution is used before the application of the high adhesive double sided. The sensor is then bonded to the top side of the tape. The film output charges are measured using alligator clips on the patches tabs and BNC connectors on the data acquisition unit side. Due to complexity in the fabrication of the sensor, only the on-resonance sensor of Figure 4 is fully implemented. The off-resonance sensors would have required covering the entire surface of the plate with sensor patches and thus impractical given our current fabrication process. Figure (8) shows the experimental setup. A 6.35 mm thick aluminum plate is fastened on top of a steel frame to simulate a clamped plate. Two strips of PVDF films are bonded to the plate.

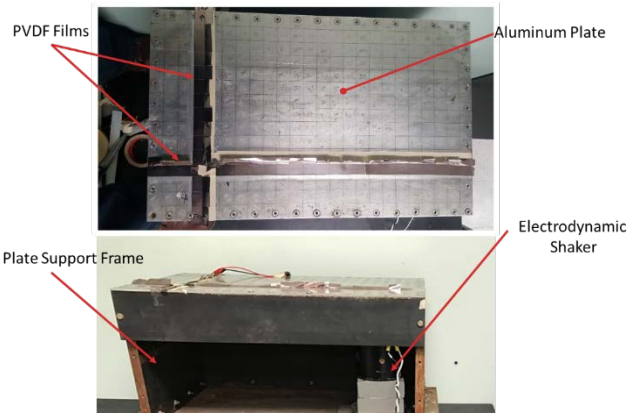

Fig. 6. Experimental setup.

The plate is excited by a Labworks ET-126 shaker over a broadband of frequencies from 0-800Hz. A PCB 208C02 force gage as input and a PCB 355B03 accelerometer as output are used to measure the plate Frequency Response Functions (FRF) over a grid drawn on the plate as seen in Figure 8. During the measurement the location of the excitation force is fixed but the accelerometer position is move over the grid and FRF at center of each grid box is recorded. Three hundred and sixty (360) accelerances are measured with the accelerometer [25]. The same process is repeated for the PVDF patches moving the alligator clips from one tab to the next. A total of 39 FRFs are recorded using the output charge of each patch of the sensor strips.

The accelerance data is processed as follows. Assuming the motion to be harmonic at each frequency, the plate admittances are calculated at each measurement point by dividing the accelerance measurements by $-\omega_i^2$ where i is the i^{th} frequency within the excitation broadband frequency. The admittances are then converted in displacement by setting the excitation force to unity. Next the displacement amplitude at the first 3 natural frequencies (174 Hz, 272 Hz, and 434 Hz) at each accelerometer measurement is extracted and used to find the plate displacement curves at those frequencies. The selection of these natural frequencies are based on our observation that the sensor performance is degraded at higher frequencies. For the PVDF measurements, the charges of each patch are used to calculate the admittances along the film strips using Equations (21), (22), (23), and (24). Again, assuming a unit force input, the admittances are converted in displacement and Equation (25) is used to calculate the plate displacement curves at the previously selected resonance frequencies. The results are shown in Figure 9.

Figure 9a shows the displacements along the sensor strip in the x direction from the accelerometer measurement and PVDF film measurement for the first three modes of the plates. In the figure, the stars represent the displacements calculated from accelerometer measurements while the continuous lines are from the PVDF sensor. Similar plots (not shown here) were

also found along the y-axis. The results indicate good agreement between the accelerometer and PVDF measurements. Obviously there are some errors that can be attributed to difficulties in the sensor fabrication process, misalignment of the sensor on the plate during bonding, but also to the mode of attachment of the PVDF film and the accelerometer. Another source of error is from the fact that the strain in the piezoelectric direction 2 is not totally eliminated. We can see on the figure that the PVDF is less accurate at the third mode. In general we observed the degradation of the PVDF sensor accuracy at higher frequency and this could be explained by the limited number of film patches and the fact that the shaker was not able to excite higher frequencies to create measureable strains. Figure 9b, c, and d are generated from the data of Figure 9a using Equation (20). Using the mode shape measurement along the x and y axis, the mode shape of the plate can be calculated per Raleigh theory. The errors seen in these figures have the same source as described above for the mode shape plot.

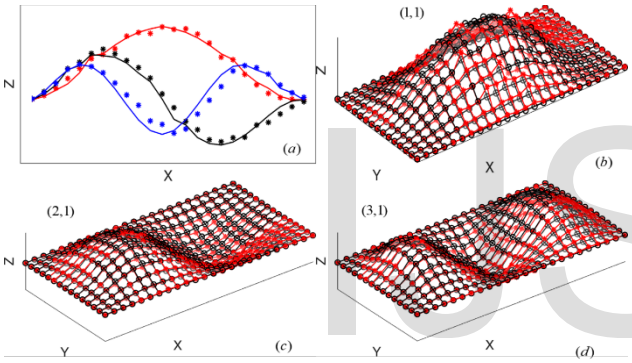

Fig. 7. Clamped plate displacement measurement. (a) Dot ="Accelerometer", Line="PVDF". (b, c, & d) Black="Accelerometer", Red="PVDF"

5 Conclusion

The paper discusses the development and implementation of PVDF film based sensor to measure the lateral displacement curve of a vibrating plate. The sensor design is an extension of previously published similar sensor for beams. The underlying equations and the physical configuration of the sensor film that can be used to measure the displacement curve of a vibrating plate are described. Two types of sensor arrangements are proposed in the paper. For measuring plate vibration deflections at resonance, two strips of sensor film are used respectively along the x and y axis of the plate. This configuration leverages Raleigh formulation of plate mode shapes as a product of beam modal shape functions to find the displacement curve of a plate vibrating at resonance. The second configuration uses sensor film patches to cover the entire surface of the plate. In either configuration, each patch measures the displacement slope at its location. These slopes are then converted into displacements or elevations, resulting in a matrix of instantaneous displacement points. The proposed sensors are validated with numerical simulations for both the general and resonance vibration cases. However for the experimental validation, only the resonance vibration case is performed. The results indicate that there is good agreement between the measurements from the sensor and those obtained with a reference accelerometer.

Two issues can be noted for the proposed sensors. The first issue is the fabrication of the sensor given the fact that the entire surface of the plate needs to be covered. However this can be overcome with additive manufacturing technology whereby the film patches can be printed on the surface of the plate. The second issue is that multiple electrodes are required to collect the outputs from the sensor patches and processed in real time. We believe that the electrodes can be printed as well on the plate between the patches and that the proposed sensor implementation can leverage miniature single chip computers as part of the sensor unit.

Finally, we believe that the proposed sensor and methodology have more far-reaching implications than simply measuring the deflection curves of a plate. But, first the study should be extended in the future to plates of arbitrary shapes because real word devices rarely have four right angles quadrilaterals. Second, it must be recognized that knowing the deflections of a dynamically loaded plate is an invaluable information that can be used in other industrial fields, for example in the development of Impact-Force-Plates for bioengineering applications and the monitoring of an aircraft skin or a race car aero package.

References

[1] Guigou, C. et al., 1997, "Active control of sound radiation using a foam-pvdf-plate passive/active composite device," International Journal of Acoustics and Vibration, 2(3), pp. 113-118

[2] Bailey, T. and Hubbard, J., 1985, "Distributed piezoelectric polymer active vibration control of a cantilever beam," Journal of Guidance, Control, and Dynamics, 8 (5), pp. 605–61

[3] Bloomfield, P. E., 1998, "Production of ferroelectric oriented PVDF films," Journal of plastic film and sheeting 4(2), 123129

[4] Miki, H. et al., 2015, "Reactive ion etching of poly (vinylidene fluoride) and its optimization," International Journal of Engineering and Technical Research, 3(3), pp. 327-333

[5] Omidi, E., Mahmoodi, S. N. J., 2015, "Multiple Mode Spatial Vibration Reduction in Flexible Beams Using H2- and H∞-Modified Positive Position Feedback," ASME Journal of Vibration and Acoustic, 137(1), pp. 011016-011016-7

[6] Adamowski, J.C., Buiochi, F., and Higuti, R.T., 2010, "Ultrasonic material characterization using large-aperture PVDF receivers," Ultrasonic, 52(2), pp. 110-115.

[7] Kryger, M., Eiken, T., and Qin, L., 2013, "The use of combined thermal/pressure polyvinylidene fluoride film airflow sensor in polysomnography," Springer-Verlag Berlin Heidelberg, pp. 1267-1273. DOI 10.1007/s11325-013-0832-5

[8] Banerjee, T. et al., 2013, "Active Control of Radiated Sound from

Stiffened Plates Using IDE-PFC Actuators," International Journal of Acoustics and Vibration, 18(3), pp. 109-116

[9] Tamjidi, et al.., 2013, "PVDF Actuator for High-Frequency Fatigue Test of Thin-Film Metals," IEEJ Transaction on Electronic and Electronic Engineering, 8, pp. 199-205.

[10] Tung, C. Y., 2015, "Precision Microscopic Actuations of Parabolic Cylindrical Shell Reflectors," ASME Journal of Vibration and Acoustic, 137(1).

[11] Lee, C. K., and Moon, F. C., 1990, ''Modal Sensors/Actuators,'' Trans. ASME, 57, pp. 434–441

[12] Clark, R. L., Flemming, M. R., and Fuller, C. R., 1993, "Piezoelectric Actuators for Distributed Vibration Excitation of Thin Plates: A Comparison between Theory and Experiment," ASME Journal of Vibration and Acoustic, 115(3), pp. 332-339.

[13] Zahui, M., Kamman, J., Naghshineh, K., 2001, "Theoretical Development and Experimental Validation of Local Volume Displacement Sensors for a Vibrating Beam," ASME Journal of Vibration and Acoustics, 123(1), pp. 110-118.

[14] Ribeiro, P., Alves, L. and Marinho, J., 2001, "Experimental Investigation on the Occurrence of Internal Resonances in a Clamped-Clamped Beam" International Journal of Acoustics and Vibration, 6(3), pp. 169-173

[15] Ding, J. et al., 2016, "Fatigue Life Assessment of Traffic-Signal Support Structures from an Analytical Approach and Long-Term Vibration Monitoring Data", J. Struct. Eng., 142(6), pp. 1-12

[16] McManus, P.S. et al., 2003, "Damping in cantilevered traffic signal structures under forced vibration," Journal of Structural Engineering, 129(3), pp.373-382

[17] Rao, S., 2004, Mechanical vibrations, Addison-Wesley 4th edition.

[18] Salo J., Korhonen I., 2014, "Calculated estimate of FBG sensor's suitability for beam vibration and strain measuring," Measurement, 47, pp. 178-173.

[19] Tzou, H. S., 1993, Piezoelectric Shells, Kluwer Academic Publishers, Dordrecht, Boston, London.

[20] Feng, K., Shi, Z., 1981, Mathematical Theory of Elastic Structures, Springer New York, ISBN 0-387-51326-4.

[21] Zahui, M., and Thomas, R., 2014, "Design of Beam Surface Displacement Sensors," ASME International Mechanical Engineering Conference and Exposition 2014, 1–7.

[22] Zahui, M and Rohan, T, 2017, "Beam Vibration Displacement Curve Measurement" International Journal of Acoustics and Vibration, 22(1), pp. 111-120.Vibration, 6(3), pp. 169-173

[23] Leissa, A. W., 1969, Vibration of Plates, NASA SP- 160.

[24] Zahui, M., and Pinjan, A., "Plate Vibration Displacement Curve Measurement", 25th International Congress on Sound and Vibration, Hiroshima, Japan, (2018).

[25] Ewins, D. J., 1984, Modal Testing: Theory, Practice and Application 2nd Edition, research Studies Press Ltd, Baldock, Hertfordshire, England.